This article has been accepted for inclusion in a future issue of this journal. Content is final as presented, with the exception of pagination.

Design of an Integral Suboptimal Second-Order Sliding Mode Controller for the Robust Motion Control of Robot Manipulators

Antonella Ferrara, *Senior Member, IEEE*, and Gian Paolo Incremona, *Member, IEEE*

***Abstract*— The formulation of an *integral suboptimal second-order sliding mode* ((ISSOSM) control algorithm, oriented to solve motion control problems for robot manipulators, is presented in this paper. The proposed algorithm is designed so that the so-called *reaching phase*, normally present in the evolution of a system controlled via the sliding mode approach, is reduced to a minimum. This fact makes the algorithm more suitable to be applied to a real industrial robot, since it enhances its robustness, by extending it also to time intervals during which the classical sliding mode is not enforced. Moreover, since the algorithm generates second-order sliding modes, while the model of the controlled electromechanical system has a relative degree equal to one, the control action actually fed into the plant is continuous, which provides a positive chattering alleviation effect. The assessment of the proposal has been carried out by experimentally testing it on a COMAU SMART3-S2 anthropomorphic industrial robot manipulator. The satisfactory experimental results, also compared with those obtained with a standard proportional-derivative controller and with the original suboptimal algorithm, confirm that the new algorithm can actually be used in an industrial context.**

***Index Terms*— Nonlinear control systems, robot control, robust control, sliding mode control (SMC), uncertain systems.**

I. INTRODUCTION

SLIDING MODE CONTROL (SMC) is a widely used control methodology that ensures good performance of the controlled system even in the presence of a significant class of uncertainties [1], [2]. Yet, because of the discontinuous nature of the SMC law, it can produce the so-called chattering effect [3]–[6], i.e., high-frequency oscillations of the controlled variable, which can be disruptive for the controlled plant, or significantly limit the life cycle of the actuators. This is the reason why the use of SMC in robotics is quite limited. Spong *et al.* [7, Sec. 8.4.11] suggested, in order to control robotic systems, to implement a continuous approximation of the discontinuous control, which, however, could only guarantee the uniformly ultimately boundedness of the tracking error. This, in practice, diminishes the efficacy of SMC, since a pseudo-sliding mode is generated, rather than an ideal sliding mode, and the robustness features of the methodology are lost. In spite of this, in the literature, the application of SMC to mechanical systems has been illustrated through a variety of examples, for both control (see [8]–[11], and the references therein indicated) and state observation [12]–[14].

Nowadays, a well-established method to perform chattering alleviation is that of consisting in confining the discontinuity, necessary to ensure the finite-time zeroing of the so-called sliding variable, to a derivative of the control variable so that the control signal actually fed into the plant is continuous. This approach, called higher order sliding mode (HOSM) control [15]–[21], after a transient phase, enforces a sliding mode involving not only the sliding variable but also its time derivatives up to the order $\rho - 1$ (the mode is accordingly called ρ-sliding mode).

Because of the continuous nature of the control action, the HOSM control approach is appropriate to be applied even to electromechanical or mechanical systems [22], [23], as testified by [24], [26] and Capisani and Ferrara [25]. Yet, as highlighted in [17], some problems remain during the transient phase, the so-called *reaching phase*, since in that time interval, which proves to be of finite but, in general, unpredictable length, the robustness properties of the control approach do not hold.

In this paper, inspired by [27], we propose a modification of the control algorithm considered in [24], which belongs to the class of the so-called suboptimal second-order sliding mode (SSOSM) algorithms [15], [17]. It gives rise to a new version of the algorithm, herein named *integral SSOSM* (ISSOSM) algorithm. The proposed algorithm maintains the good properties of the original SSOSM approach in terms of chattering alleviation but also assigns a transient dynamics to the controlled system so that the reaching phase occurs with a prescribed transient time. This feature is highly beneficial in robotics, since it limits the time periods during which the two-sliding mode on the selected sliding manifold is not enforced.

In fact, the integral two-sliding mode is attained on a suitably modified sliding manifold from the initial time instant (this time instant being the time instant when the adopted Levant's differentiator [28], [29], involved in the scheme, converges), and from that time instant, the robustness of the controlled system can be proved. This implies that the guaranteed robustness is enhanced with respect to that provided by the conventional SSOSM algorithm, which makes

Manuscript received June 17, 2014; revised December 28, 2014; accepted March 22, 2015. Manuscript received in final form March 27, 2015. Recommended by Associate Editor N. van de Wouw.

The authors are with the Dipartimento di Ingegneria Industriale e dell'Informazione, University of Pavia, Pavia 27100, Italy (e-mail: antonella.ferrara@unipv.it; gp.incremona@gmail.com).

Color versions of one or more of the figures in this paper are available online at http://ieeexplore.ieee.org.

Digital Object Identifier 10.1109/TCST.2015.2420624

This article has been accepted for inclusion in a future issue of this journal. Content is final as presented, with the exception of pagination.

the new algorithm more suitable to be applied to real industrial robots.

The effectiveness of the proposed approach has been assessed experimentally, relying on a COMAU SMART3-S2 anthropomorphic industrial robot manipulator. The comparison based on experimental tests with the results obtained using a standard proportional-derivative (PD) controller and the original suboptimal algorithm shows the superiority of the present proposal and confirms its applicability in an industrial context. Note that a preliminary version of this paper, not reporting the proofs of the results and only including simulations, has been published in [30].

This paper is organized as follows. In Section II, the concepts underlying HOSM control, second-order SMC, and integral SMC are briefly revised for the readers' convenience. The new algorithm is presented and analyzed in Section III. Section IV is devoted to discuss the case study: the kinematical and dynamical models of the three-joints planar robot manipulator used in the experimental tests are illustrated, and the design of a motion control scheme based on the use of the proposed ISSOSM algorithm is discussed in detail. Finally, the experimental results are reported together with the aforementioned comparison. Some conclusions, gathered in Section V, end this paper.

II. Some Preliminary Issues

Consider the single-input single-output (SISO) system given by

$$\begin{cases} \dot{x}_i(t) = x_{i+1}(t), \quad i = 1, \dots, n-1 \\ \dot{x}_n(t) = f(\boldsymbol{x}(t)) + g(\boldsymbol{x}(t))u(t) \\ y(t) = s(\boldsymbol{x}(t)) \end{cases} \tag{1}$$

where $\boldsymbol{x}(t) \in \mathbb{R}^n$ is the state vector, $u(t) \in \mathbb{R}$ is the control variable, and $s : \mathbb{R}^n \to \mathbb{R}$ is a smooth output function, named *sliding variable* in the subsequent analysis. System (1) is an *uncertain system* since f and g are assumed to be unknown smooth functions. The *relative degree* of the system, i.e., the minimum order r of the time derivative $s^{(r)}$ of the sliding variable in which the control u explicitly appears, is considered well defined, uniform, and time invariant. In the following, the dependence of s on $\boldsymbol{x}(t)$ and of all the variables on t is omitted in some cases, when it is obvious, for the sake of simplicity.

A. Higher Order Sliding Mode Control

The HOSM control problem is based on the definition of an *auxiliary system* associated with the original uncertain system. The auxiliary system is a perturbed chain of integrators built starting from the sliding variable and its time derivatives. Thus, the original control objective, attained in conventional SMC by zeroing the sliding variable in finite time, is transformed into the aim of finite time regulating the auxiliary system. This means to force the system state to reach in finite time the subspace named *ρ-sliding manifold* $s = \dot{s} = \cdots = s^{(\rho-1)} = 0$, for any ρth order sliding mode control (ρ being the relative degree of the auxiliary system such that $\rho \geq r$ and $\rho \geq 2$), and there remain for any subsequent time instant. The time derivative $s^{(\rho)}$ is the bounded function, which, relying on (1), can be expressed as follows:

$$s^{(\rho)}(\boldsymbol{x}(t)) = F(\boldsymbol{x}(t), u(t)) + g(\boldsymbol{x}(t))w(t) \tag{2}$$

where $F = s^{(\rho)}|_{w=0}$ and $g = (\partial s^{(\rho)}/\partial u) \neq 0$ are the unknown functions and w is a new control variable. Note that if the relative degree of the auxiliary system is such that $\rho = r + 1$, i.e., an artificial increment of the relative degree is performed to build the auxiliary system, then $w = \dot{u}$, and F depends on u; while if the relative degree is $\rho = r$, then $w = u$ and the function F does not depend on u. To prove, using standard argumentations, the finite time convergence of the auxiliary system state to zero, F and g are assumed to be bounded. More precisely, one has that there exist positive constants G_1, G_2, and F_0 such that

$$0 < G_1 \leq g(\boldsymbol{x}(t)) \leq G_2 \tag{3}$$

$$|F(\boldsymbol{x}(t), u(t))| \leq F_0. \tag{4}$$

Note that instead of (3), one could analogously have the opposite inequality

$$-G_2 \leq g(\boldsymbol{x}(t)) \leq -G_1 < 0 \tag{5}$$

i.e., it is required that function g has constant known sign. Since the information about the bounds of F and g are assumed to be available, the original dynamical system (1) implies the differential inclusion [31]

$$s^{(\rho)} \in [-F_0, F_0] + [G_1, G_2]w. \tag{6}$$

In the literature, it has been shown that the problem of making the ρ-sliding manifold associated with (6) finite-time attractive, generating a sliding mode of order ρ (ρ-sliding mode), can be solved by any ρ-sliding mode controller of the type [16]–[21]

$$u(t) = U_{\max}\Psi(s, \dot{s}, \dots, s^{(\rho-1)}) \tag{7}$$

where Ψ is a discontinuous function and $U_{\max} > 0$ is chosen so as to ensure the finite-time convergence of the state trajectories.

B. Second-Order Sliding Mode Control

Second-order sliding mode (SOSM) control is a particular case of HOSM control. Assume that the sliding variable is chosen as

$$s(\boldsymbol{x}(t)) = x_n(t) + \sum_{i=1}^{n-1} m_i x_i(t) \tag{8}$$

where $m_i, i = 1, \dots, n-1$ are the real positive constants. Because of the foregoing sliding variable choice, the auxiliary system turns out to be, in our case, a relative degree one system. Yet the use of a control law (7) discontinuous on $s = 0$ is not appropriate for an electromechanical application, because of the chattering effect that it can induce [22]. Then, it is convenient to artificially increase the relative degree of the auxiliary system, as suggested in [17]. To this end,

Algorithm 1 SSOSM Algorithm

1) Set $\xi_1(t) = s(\boldsymbol{x}(t))$ and $\xi_2(t) = \dot{s}(\boldsymbol{x}(t))$.
   Repeat for any $t > t_0$, the following steps.
2) Set $\alpha^* \in (0,1] \cap (0, 3G_1/G_2)$.
3) Set $\xi_{1_{max}} = \xi_1(t_0)$.
4) If $\left[\xi_1(t) - \frac{1}{2}\xi_{max}\right][\xi_{max} - \xi_1(t)] > 0$, then set $\alpha = \alpha^*$, else set $\alpha = 1$.
5) If $\xi_1(t)$ is extremal, the set $\xi_{max} = \xi_1(t)$.
6) Apply the control law

$$w(t) = -\alpha U_{max} \operatorname{sgn}\left(\xi_1(t) - \tfrac{1}{2}\xi_{max}\right) \tag{12}$$

with

$$U_{max} > \max\left(\frac{F_0}{\alpha^* G_1}; \frac{4F_0}{3G_1 - \alpha^* G_2}\right) \tag{13}$$

one has to consider the first- and the second-time derivative of the sliding variable

$$\dot{s}(\boldsymbol{x}(t)) = f(\boldsymbol{x}(t)) + g(\boldsymbol{x}(t))u(t) + \sum_{i=1}^{n-1} m_i x_{i+1}(t) \tag{9}$$

$$\begin{aligned}\ddot{s}(\boldsymbol{x}(t)) = {} & \frac{d}{dt} f(\boldsymbol{x}(t)) + \frac{d}{dt} g(\boldsymbol{x}(t))u(t) + g(\boldsymbol{x}(t))\dot{u}(t) \\ & + m_{n-1}[f(\boldsymbol{x}(t)) + g(\boldsymbol{x}(t))u(t)] + \sum_{i=1}^{n-2} m_i x_{i+2}(t).\end{aligned} \tag{10}$$

By defining $\xi_1(t) = s(\boldsymbol{x}(t))$ and $\xi_2(t) = \dot{s}(\boldsymbol{x}(t))$, it yields

$$\begin{cases} \dot{\xi}_1(t) = \xi_2(t) \\ \dot{\xi}_2(t) = F(\boldsymbol{x}(t), u(t)) + g(\boldsymbol{x}(t))w(t) \end{cases} \tag{11}$$

where $\xi_2(t)$ is assumed to be unmeasurable, functions F and g have the bounds indicated in (3) and (4), and $w(t)$ is the auxiliary control law that has to be designed so that $\xi_1(t)$ and $\xi_2(t)$ are steered to zero in a finite time in spite of the uncertainties, thus enforcing an SOSM. Note that F in (10) depends on the state $x_3, \ldots, x_n$, so that it is only locally bounded, which is true in most practical cases, since the operational region is always bounded. Moreover, according to (7), the control $w(t) = \dot{u}(t)$ is discontinuous. Yet, by virtue of the artificial increment of the relative degree, the control actually fed into the plant is the output of an integrator having in input $w(t)$ that is it is continuous, which is highly appreciable in case of mechanical or electromechanical plants. Note that in the literature, several algorithms have been proposed to solve second-order sliding mode control problems, such as the twisting and supertwisting algorithms [32], and the suboptimal algorithm [15], [17]. In this paper, we will use the suboptimal algorithm as an ingredient of the proposed control scheme. Therefore, for the readers' convenience, the SSOSM algorithm is reported in Algorithm 1. Note that, F linearly depends on u, which, in principle, does not ensure its boundedness. Since, in the present approach, an SOSM $s = \dot{s} = 0$ is enforced, the control u is close to the so-called equivalent control $u_{\mathrm{eq}}(\boldsymbol{x}, t)$, obtained by posing $\dot{s}(\boldsymbol{x}, u_{\mathrm{eq}}, t) = 0$ [1], [33], and one can conclude that the control law (12), (13) is locally applicable.

C. Integral Sliding Mode Control

Recent research has been devoted to studying integral sliding mode (ISM) methods, which enable to generate an ideal sliding mode of the controlled system on a particular sliding manifold starting from the initial time instant t_0 that is eliminating the so-called reaching phase, which can be beneficial for robustness issues. A sliding mode is defined integral if the system, while in sliding, is of the same order as the original system [34]. ISM requires splitting the control variable into two parts

$$u(t) = u_0(t) + u_1(t) \tag{14}$$

where $u_0(t)$ is generated by a suitable controller designed relying on the nominal plant, and $u_1(t)$ is a discontinuous control action designed to compensate for the uncertainties affecting the system. A particular sliding manifold is defined, named *integral sliding manifold*, as

$$\Sigma(t) = s(\boldsymbol{x}(t)) - \varphi(t) = 0 \tag{15}$$

where Σ is the auxiliary sliding variable, s is the actual sliding variable, chosen, for instance, as in (8), and the integral term φ is given by

$$\varphi(t) = s(\boldsymbol{x}(t_0)) + \int_{t_0}^{t} \frac{\partial s}{\partial \boldsymbol{x}} \dot{\boldsymbol{x}}(\zeta) d\zeta \tag{16}$$

with the initial condition $\varphi(t_0) = s(\boldsymbol{x}(t_0))$. By virtue of the choice of $\varphi(t)$ and $\varphi(t_0)$, it is apparent that the controlled system is in sliding mode on the manifold $\Sigma(t) = 0$ since the initial time instant. This affects the robustness features of the controlled system, as will be discussed, with reference to the robotic case in the next section.

III. New Proposal: Integral Suboptimal Second-Order Sliding Mode

In this section, an integral version of the SSOSM algorithm, named ISSOSM, is presented. This new control approach maintains the good properties of the original suboptimal algorithm in terms of capability of stabilizing in finite time a perturbed chain of integrators with bounded control, as well as in terms of chattering alleviation. Moreover, the reaching phase is reduced to a minimum, as will be clarified in a moment, by the introduction of transient dynamics with a prescribed time.

Consider the auxiliary sliding variable $\Sigma(t)$ in (15). Assume being able to generate a sliding mode on $\Sigma = 0$ since the initial time instant t_0. If t_f is the time instant when the condition $s = 0$ is attained, then

$$s(t) = \varphi(t) \quad \forall t, \ t_0 \le t \le t_f. \tag{17}$$

By chosing, according to [27], the transient function $\varphi(t)$ as

$$\begin{cases} \varphi(t) = (t - t_f)^2 (c_0 + c_1(t - t_0)) & \forall t, \quad t_0 \le t \le t_f \\ \varphi(t) = 0 & \forall t > t_f \\ \varphi(t_0) = s(t_0), & \dot{\varphi}(t_0) = \dot{s}(t_0) \end{cases} \tag{18}$$

one has that the design parameters c_0 and c_1 can be determined as follows:

$$c_0 = s(t_0)T^{-2} \tag{19}$$

$$c_1 = \dot{s}(t_0)T^{-2} + 2s(t_0)T^{-3} \tag{20}$$

This article has been accepted for inclusion in a future issue of this journal. Content is final as presented, with the exception of pagination.

Algorithm 2 ISSOSM Algorithm

1) Set $\Sigma(t) = s(\boldsymbol{x}(t)) - \varphi(t)$, $\xi_1(t) = \Sigma(t)$ and $\xi_2(t) = \dot{\Sigma}(t)$.
   Repeat for any $t > t_0$, the following steps.
2) Set $\alpha^* \in (0,1] \cap (0, 3G_1/G_2)$.
3) Set $\xi_{1_{max}} = \xi_1(t_0)$.
4) If $t_0 \le t \le t_f$, then set $\varphi(t) = (t - t_f)^2(c_0 + c_1(t - t_0))$, else set $\varphi(t) = 0$.
5) If $\left[\xi_1(t) - \frac{1}{2}\xi_{max}\right][\xi_{max} - \xi_1(t)] > 0$, then set $\alpha = \alpha^*$, else set $\alpha = 1$.
6) If $\xi_1(t)$ is extremal, the set $\xi_{max} = \xi_1(t)$.
7) Apply the control law (12) with (13).

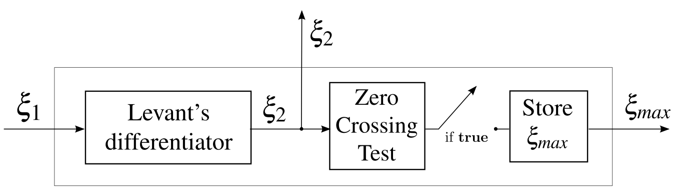

Fig. 1. Peak detection block scheme to evaluate the extremal value $\xi_{\max}$ in the ISSOSM controller.

where $T = t_f - t_0$ is the so-called *prescribed convergence time*. Note that the knowledge of $\dot{s}(t_0)$ is necessary to define the transient function. Having in mind the robotic application, in which the only available sensors are resolvers capable of measuring the robot joint angular positions, we can assume that $\dot{s}$ is unmeasurable. Then, the well-known Levant's differentiator

$$\dot{z_0} = -\lambda_0 |z_0 - s|^{1/2} \operatorname{sgn}(z_0 - s) + z_1 \tag{21}$$

$$\dot{z_1} = -\lambda_1 \operatorname{sgn}(z_0 - s) \tag{22}$$

where z_0 and z_1 are the estimated values of s, $\dot{s}$, respectively, and $\lambda_0 = L^{1/2}$, $\lambda_1 = 1.1L$, $L \ge F + \sup|\ddot{s}|$, is a possible choice of the differentiator parameters [28], is introduced in the control scheme. It is used for an initialization time period ending in t_0, with $t_0 \ge t_d$, t_d being the differentiator convergence time or an upper bound of it.

With reference to the SSOSM algorithm [17], mentioned in the previous section, considering the sliding variable used to define the integral sliding manifold $\Sigma = s - \varphi$, and the auxiliary system (11) with $\xi_1 = \Sigma$ and $\xi_2 = \dot{\Sigma}$, Algorithm 2 can be written. Since the ISSOSM control law depends on the auxiliary sliding variable Σ, the control u is bounded along the integral sliding mode trajectory $\Sigma = \dot{\Sigma} = 0$ from the initial time instant t_0, and, with bounds (3) and (4), it results in being semiglobally applicable.

Remark 1: Note that a possibility to evaluate the extremal values $\xi_{\max}$ can be to use a device of the type shown in Fig. 1. In practice, this means that even if the state $\dot{\Sigma}$ is not available for measurements, it can be estimated by the robust differentiator, the structure of which is reported in (21) and (22), and the extremal values of $\Sigma(t)$ can be stored at the time instant when $\dot{\Sigma}(t)$ changes its sign. In alternative, one can deduce $\dot{\Sigma}$ relying on the definition of Σ and on the estimate of $\dot{s}$ obtained through (21) and (22).

With reference to the proposed control approach, the following results can be proved.

Theorem 1: Given system (1), the auxiliary system (11) with bounds as in (3) and (4), and this latter controlled via the ISSOSM algorithm, the convergence of the auxiliary system trajectories to the origin of the state plane takes place in a finite time. Moreover, given the transient function (18), an integral sliding mode is enforced on the integral sliding manifold $\Sigma(t) = 0$ introduced in (15) $\forall t,\ t \ge t_0$, t_0 being the initial time instant. In addition, $\forall t \ge t_f$, one has that the origin of the original system, i.e., system (1), results in being an exponentially stable equilibrium point.

Proof: The proof of the fact that the convergence to the origin of the auxiliary system state plane occurs in a finite time relies on the proof of finite time convergence of the suboptimal controller, reported in [17]. It can be, in brief, proved that, with the constraints (13), the control law (12) enforces the generation of a sequence of states with coordinates featuring the contraction property expressed by

$$|\xi_{\max_{i+1}}| < |\xi_{\max_i}| \tag{23}$$

where $\xi_{\max_i}$ is the ith extremal value of the variable ξ_1. Moreover, let the sequence $\{t_{\max_k}\}$ denote the sequence of the time instants when an extremal value of $\Sigma(t)$ occurs, then relying on [17], it can be proved that

$$\lim_{k\to\infty} t_{\max_k} < \frac{\beta}{1-\gamma} + t_{\max_1} \tag{24}$$

where $\gamma < 1$ and

$$\beta = \sqrt{|\xi_{\max_1}|}\frac{(G_1 + \alpha^* G_2)U_{\max}}{(G_1 U_{\max} - F_0)\sqrt{\alpha^* G_2 U_{\max} + F_0}}. \tag{25}$$

Moreover, the initial conditions in (18) imply that at t_0 the auxiliary sliding variable $\Sigma(t_0) = 0$. Therefore, one has that the sliding condition is ensured in $t = t_0$. Because of the choice of the transient function φ indicated in (18), it is apparent that a sliding mode is enforced on the integral sliding manifold $\Sigma(t) = 0$ for any $t > t_0$. Then, $\Sigma(t) = 0$ for any $t \ge t_0$.

Finally, considering that $\varphi(t) = 0\ \forall t \ge t_f$, according to (18), it follows that $s(t) = 0\ \forall t \ge t_f$, that is, the integral sliding mode coincides with the conventional sliding mode since the time instant t_f. This implies, relying on (8), that

$$x_n(t) + \sum_{i=1}^{n-1} m_i x_i(t) = 0 \tag{26}$$

$\forall t \ge t_f$, so that system (1), in such time interval, can be rewritten as

$$\begin{cases} \dot{x}_i(t) = x_{i+1}(t), \quad i = 1, \ldots, n-2 \\ \dot{x}_{n-1}(t) = -\sum_{i=1}^{n-1} m_i x_i(t). \end{cases} \tag{27}$$

Since $m_i, i = 1, \ldots, n-1$ are the real positive constants, it is apparent that the free state motion of system (27) is exponentially vanishing, which concludes the proof. ■

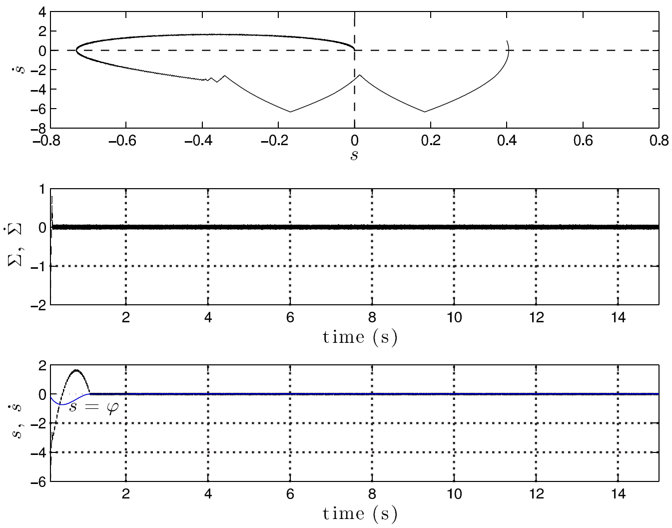

Fig. 2. Performance of a perturbed double integrator controlled via the proposed ISSOSM algorithm, with values $F_0 = 0.01$, $G_1 = G_2 = 1$, sampling time $t_s = 0.0001$ s, initial conditions $s = 0.4$, $\dot{s} = 1$, and initial time instant $t_0 = 0.1$ s to provide sufficient time for the differentiator convergence. The state space $\{s, \dot{s}\}$; the auxiliary sliding variable Σ (solid black line) and its time derivative $\dot{\Sigma}$ (dotted black line); and the sliding variable s (solid black line), and its time derivative $\dot{s}$ (dotted black line) and the transient function φ (solid blue line).

Remark 2: Note that if $\dot{\Sigma}$ were measurable, i.e., if $\dot{s}$ were available, the controlled system would be in sliding mode independently of the choice of the initial time instant t_0. Since instead a Levant differentiator is used to determine the unavailable quantities, in spite of the choice of the integral approach, it is necessary to provide sufficient time for the differentiator to converge. To diminish this differentiator time, one could consider a proper initialization of the surface, for instance, by taking into account $z_0(t_0) = s(t_0)$, $z_1(t_0) = \dot{s}(t_0) = 0$, or one can also consider a trivial rough finite-difference approximation to initialize z_1.

Note that for suitable initial conditions such that $\dot{s}(t_0) = 0$, the transient would be eliminated. Since, in the general case, the differentiator proves to converge in a finite time t_d, then one can claim that, in our case, the sliding mode is enforced for any $t \geq t_0$, with $t_0 \geq t_d$ (see Fig. 2 for an illustrative example).

By virtue of the fact that the sliding mode on the integral sliding manifold is enforced since the initial time instant, to be selected according to Remark 2, the reaching phase is eliminated, which produces a clear benefit in terms of robustness of the controlled system. In particular, starting from Theorem 1, the following theorem can be proved.

Theorem 2: Given the transient function (18), and the auxiliary sliding variable $\Sigma = s - \varphi$, upon with the integral sliding manifold (15) is defined, then system (1), controlled via the ISSOSM algorithm, is robust from the initial time instant t_0 with respect to the matched uncertainties affecting the system.

Proof: According to [34], when an integral sliding mode takes place, the system featuring this evolution mode is of the same order as the original system. If the auxiliary sliding variable is chosen as $\Sigma(t) = s(t) - \varphi(t)$, since Theorem 1 proves that the sliding mode is enforced on $\Sigma = 0$ since the initial time instant, during the time interval $t_0 \leq t \leq t_f$,

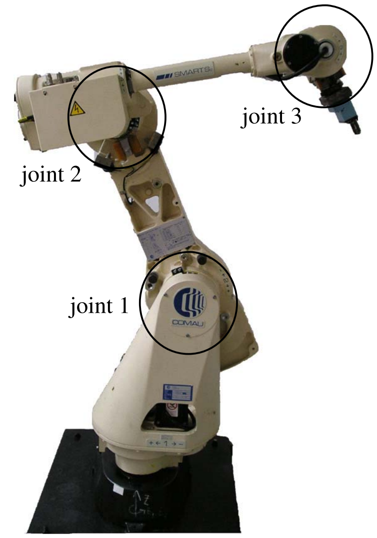

Fig. 3. COMAU SMART3-S2 anthropomorphic industrial robot manipulator used for the experimental tests with the joints' numeration.

one has that the equivalent system dynamics (see [1] for a definition) is given by

$$\begin{cases} \dot{x}_i(t) = x_{i+1}(t), \quad i = 1, \ldots, n-2 \\ \dot{x}_{n-1}(t) = -\sum_{i=1}^{n-1} m_i x_i(t) + \varphi(t) \\ \dot{\varphi}(t) = \dot{\varphi}(t_0) + \int_{t_0}^{t} \ddot{\varphi}(\zeta) dt d\zeta \end{cases} \tag{28}$$

where $\ddot{\varphi}(t)$ is known and bounded by construction, since $\varphi(t)$ is arbitrarily designed. It is apparent that the equivalent system is invariant, even if the original system is affected by matched uncertainties. Moreover, for $t > t_f$, system (28) is transformed into system (27), which again does not depend on the uncertainty terms. Then the controlled system evolution is invariant with respect to the evolution of the uncertainty terms affecting system (1) and such a robustness property holds for $\forall t \geq t_0$, which proves the theorem. ■

IV. Case Study

In this section, the results of the experimental verification and validation of the proposed algorithm are reported. During the experimental tests, for the sake of simplicity, only vertical planar motions of the robot manipulator were enabled, by locking three of the six joints of the robot (Fig. 3), so that the schematic view of the considered robot is the one in Fig. 5. This was done to make it possible to adopt as a control design model, the robot model identified in [35]. Indeed, the proposed control approach is valid for any n-degree of mobility robot manipulator, even of spatial type.

A. Robot Model

Consider Fig. 4. Let $l_i, i = 1, 2, 3$, denote the length of the ith link, q_1 the orientation of the first link with respect to $\boldsymbol{y}$-axis, clockwise positive, and let q_j, $j = 2, 3$, denote the displacement of the jth link with respect to the $(j-1)$th one, clockwise positive. Let $O - \{\boldsymbol{x}, \boldsymbol{y}, \boldsymbol{z}\}$ be the base-frame for the robotic manipulator so that the center O is placed in the center of the first joint of the robot. Let $O_e - \{\boldsymbol{n}, \boldsymbol{s}, \boldsymbol{a}\}$ be the

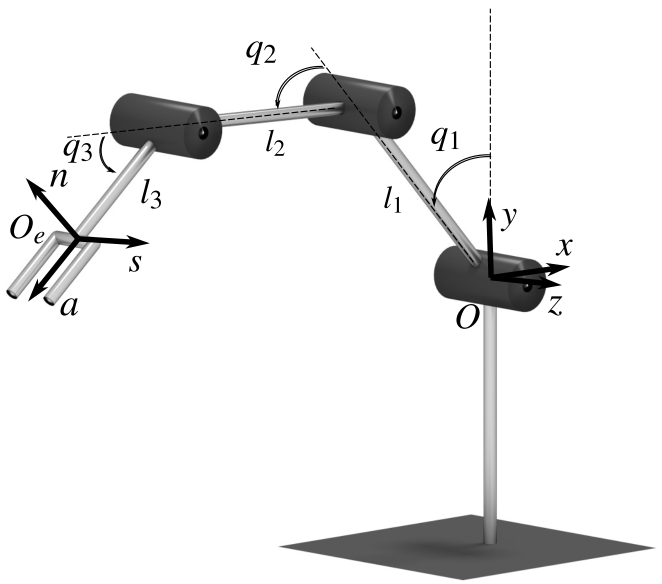

Fig. 4. Spatial schematic view of the considered three-joint robotic manipulator.

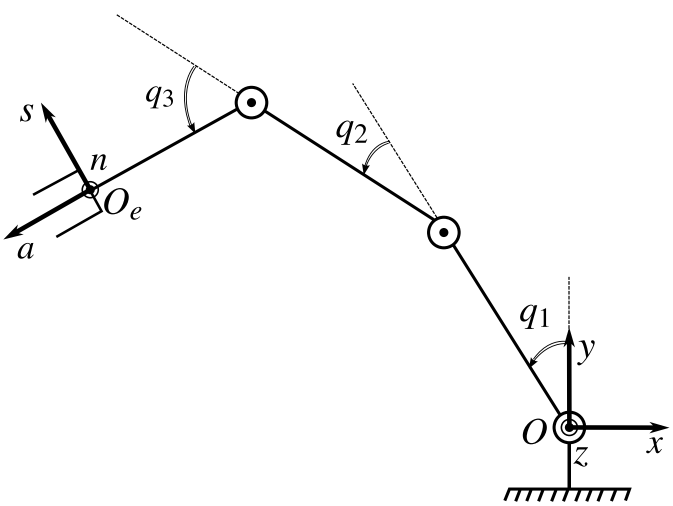

Fig. 5. Schematic planar view of the robot manipulator with the joint variables.

end-effector frame so that the center O_e is placed on the robot end-effector, and the axes $\{\boldsymbol{n}, \boldsymbol{s}, \boldsymbol{a}\}$ are shown in Fig. 4.

The direct kinematics of a three-joints planar manipulator describes the relationship between the joint variables $\boldsymbol{q} = [q_1\ q_2\ q_3]^T$ and the end-effector position and orientation $\boldsymbol{x} = [p_x\ p_y\ \phi]^T$ in the planar workspace, which is plane in this case. With reference to Fig. 5, where the joint variables $q_i, i = 1, 2, 3$ are indicated, the direct kinematics equations, in the considered case, can be written as

$$\begin{cases} p_x = -l_1 \sin(q_1) - l_2 \sin(q_1 + q_2) - l_3 \sin(\phi) \\ p_y = l_1 \cos(q_1) + l_2 \cos(q_1 + q_2) + l_3 \cos(\phi) \\ \phi = q_1 + q_2 + q_3. \end{cases} \tag{29}$$

The dynamics of the robot can be described in the joint space, using the Lagrangian approach, as

$$\boldsymbol{B}(\boldsymbol{q})\ddot{\boldsymbol{q}} + \boldsymbol{n}(\boldsymbol{q}, \dot{\boldsymbol{q}}) = \boldsymbol{\tau} \tag{30}$$

$$\boldsymbol{n}(\boldsymbol{q}, \dot{\boldsymbol{q}}) = \boldsymbol{C}(\boldsymbol{q}, \dot{\boldsymbol{q}})\dot{\boldsymbol{q}} + \boldsymbol{F}_v\dot{\boldsymbol{q}} + \boldsymbol{F}_s\mathbf{sgn}(\dot{\boldsymbol{q}}) + \boldsymbol{g}(\boldsymbol{q}) \tag{31}$$

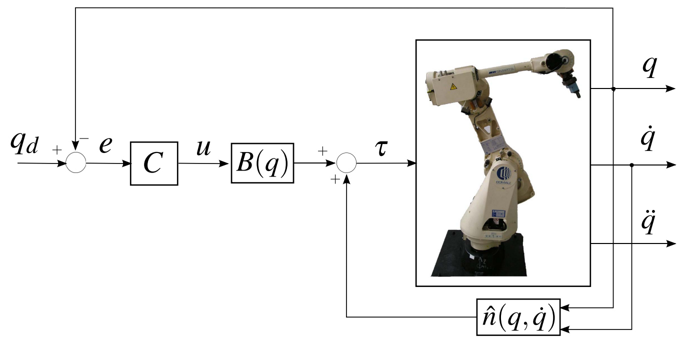

Fig. 6. Motion control scheme with the inverse dynamics-based feedback linearization applied to the robot system.

where $\boldsymbol{B}(\boldsymbol{q}) \in \mathbb{R}^{3\times3}$ is the inertia matrix, $\boldsymbol{C}(\boldsymbol{q}, \dot{\boldsymbol{q}}) \in \mathbb{R}^{3\times3}$ represents centripetal and Coriolis torques, $\boldsymbol{F}_v \in \mathbb{R}^{3\times3}$ is the viscous friction matrix, $\boldsymbol{F}_s \in \mathbb{R}^{3\times3}$ is the static friction matrix, $\boldsymbol{g}(\boldsymbol{q}) \in \mathbb{R}^3$ is the vector of gravitational torques and $\boldsymbol{\tau} \in \mathbb{R}^3$ represents the motors torques. Note that the static friction is neglected during the design of the ISSOSM controller, but it is obviously present in the actual industrial robot during the experimental tests.

B. Motion Control Scheme

In Fig. 6, the proposed control scheme is illustrated. The feedback loop is designed for the joint angular position tracking control, the desired joint positions being compared with the real positions. Controller C computes the control variable $\boldsymbol{u} \in \mathbb{R}^3$ starting from the position error $\boldsymbol{e} \in \mathbb{R}^3$ with

$$\boldsymbol{e} = \boldsymbol{q}_d - \boldsymbol{q}. \tag{32}$$

To feedback linearize the nonlinear system (30), the classical inverse dynamic control approach [36] has been adopted to create a suitable internal loop. The inverse dynamics of a rigid robot manipulator can be written in the joint space as a nonlinear relationship between the plant inputs and the plant outputs, relying on (30) and (31), so that the control law results in

$$\boldsymbol{\tau} = \boldsymbol{B}(\boldsymbol{q})\boldsymbol{u} + \hat{\boldsymbol{n}}(\boldsymbol{q}, \dot{\boldsymbol{q}}) \tag{33}$$

where $\boldsymbol{u}$ is an auxiliary control variable. Note that $\boldsymbol{B}(\boldsymbol{q})$ and $\hat{\boldsymbol{n}}$ need to be identified on the basis of experimental tests. In this paper, we assume that the identified matrix $\boldsymbol{B}(\boldsymbol{q})$ coincides with the actual one (or it is a quite accurate replica), which, on the basis of our experience, is often true in practice, while $\hat{\boldsymbol{n}}$ is an estimate of $\boldsymbol{n}$, which does not necessarily coincide with $\boldsymbol{n}$. In the following, we make reference to the experimentally identified $\boldsymbol{B}(\boldsymbol{q})$ and $\hat{\boldsymbol{n}}$ in [35].

By applying the feedback linearization to system (30) and (31), one obtains

$$\ddot{\boldsymbol{q}} = \boldsymbol{u} + \boldsymbol{B}^{-1}(\boldsymbol{q})\tilde{\boldsymbol{n}}(\boldsymbol{q}, \dot{\boldsymbol{q}}) = \boldsymbol{u} - \boldsymbol{\eta}(\boldsymbol{q}, \dot{\boldsymbol{q}}) \tag{34}$$

where $\boldsymbol{\eta}(\boldsymbol{q}, \dot{\boldsymbol{q}}) = \boldsymbol{B}^{-1}(\boldsymbol{q})\tilde{\boldsymbol{n}}(\boldsymbol{q}, \dot{\boldsymbol{q}})$ takes into account modeling uncertainties and unmodeled dynamical effects and

$$\tilde{\boldsymbol{n}}(\boldsymbol{q}, \dot{\boldsymbol{q}}) = \hat{\boldsymbol{n}}(\boldsymbol{q}, \dot{\boldsymbol{q}}) - \boldsymbol{n}(\boldsymbol{q}, \dot{\boldsymbol{q}}). \tag{35}$$

This means that the whole system is reduced to the juxtaposition of three decoupled uncertain SISO systems. Because of physical constraints, the uncertain term affecting any single system can be regarded as a bounded term. Proceeding experimentally, it is possible to evaluate the bound magnitude so that it can be assumed that $|\eta_i| < H_i$, η_i being the ith component of $\boldsymbol{\eta}(\boldsymbol{q}, \dot{\boldsymbol{q}})$.

Now we design controller C relying on the previously described ISSOSM approach. According to this latter, a sliding variable for each SISO system is selected as

$$s_i(t) = m_i e_i(t) + \dot{e}_i(t), \quad i = 1, 2, 3 \tag{36}$$

where $m_i \in \mathbb{R}$ is scalar and e_i is the position error of the ith joint. The relative degree of each SISO system involving a single sliding variable s_i (considering s_i as the relevant system output) is equal to $r = 1$, so that the control variable appears in the first time derivative of s_i as follows:

$$\dot{s}_i(t) = m_i \dot{e}_i(t) + \ddot{e}_i(t) = m_i \dot{e}_i(t) + \ddot{q}_{d_i}(t) + \eta_i(t) - u_i(t) \tag{37}$$

and the discontinuous auxiliary control $w_i(t)$ only affects $\ddot{s}_i$. Relying on the theoretical treatment in Section III, the transient function φ_i is chosen as in (18), while the auxiliary sliding variable defining the integral sliding manifold for each joint is $\Sigma_i = s_i - \varphi_i$. The auxiliary system, with relative degree $\rho = 2$, can be written as

$$\begin{cases} \dot{\xi}_{1_i}(t) = \xi_{2_i}(t) \\ \dot{\xi}_{2_i}(t) = m_i(\ddot{q}_{d_i}(t) + \eta_i(t) - u_i(t)) + \dfrac{d^3 q_{d_i}(t)}{dt^3} + \dot{\eta}_i(t) \\ -w_i(t) - \ddot{\varphi}_i(t) \end{cases} \tag{38}$$

where $\xi_{1_i}(t) = \Sigma_i$ and $\xi_{2_i}(t) = \dot{\Sigma}_i$, while $w_i = \dot{u}$ is the discontinuous control law. The auxiliary control law $w(t)$ is chosen as (12) in the ISSOSM algorithm statement, while the effective control variable is

$$u_i(t) = \int_0^t \alpha_i U_{\max_i} \operatorname{sgn}\left(\xi_{1_i}(\zeta) - \frac{1}{2}\xi_{\max_i}\right) d\zeta \tag{39}$$

which is continuous. This way to confine discontinuity in the first time derivative of the control signal is normally regarded as a chattering alleviation approach in the SMC literature.

C. Experimental Results

The proposed control approach has been verified by performing experimental tests on a COMAU SMART3-S2 industrial anthropomorphic rigid robot manipulator (Fig. 3). The SMART3-S2 robot consists of six links and six rotational joints driven by brushless electric motors, but only three joints have been used in the tests, as previously mentioned. To acquire the joints positions, resolvers are fastened on the three motors. The controller has a sampling time equal to $t_s = 0.001$ s.

Note that the performance obtained during experiments are comparable with the results attained in simulation, as published in [30]. Hereafter, for the sake of brevity, only the parametric and initial values of the algorithm applied

TABLE I
CONTROL PARAMETERS (SIMULATION)

i	m_i	α_i^*	U_{max_i}
1	10	0.9	630
2	10	0.9	2130
3	10	0.9	10250

TABLE II
CONTROL PARAMETERS (EXPERIMENTS)

i	m_i	α_i^*	U_{max_i}
1	10	0.9	630
2	10	0.9	1820
3	10	0.9	15230

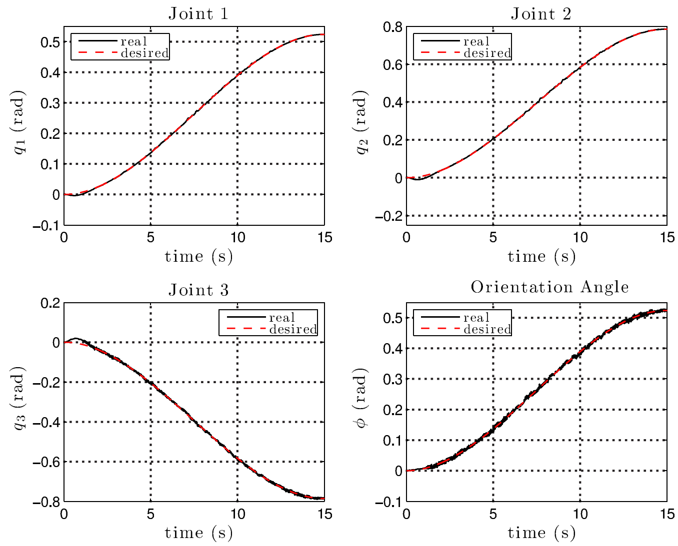

Fig. 7. Angular position of joints and end-effector orientation angle ϕ (experimental results). From the top on the left: the desired trajectory (dotted red line) and the real one (solid black line) for each joint.

in simulation are reported. The control parameters, both for simulation and experiments, are reported in Tables I and II, respectively. Note that the choice of the parameters used in simulation (which has helped us to tune the parameters in the experimental case) turns out to be conservative as for the second joint while undersized as for joint 3. This means in practice that such nonlinear effects as friction or mechanical play are not completely captured by the identified model. The goal of the control system is to steer the joint angles from a given initial position $(q_{1_0}, q_{2_0}, q_{3_0}) = (0, 0, 0)$ to the final position $(q_{1_f}, q_{2_f}, q_{3_f}) = (\pi/6,\ \pi/4,\ -\pi/4)$, following the trajectory $q_i = a_3 t^3 + a_2 t^2 + a_1 t + a_0$, where a_0, a_1, a_2, and a_3 are the coefficients depending on q_{i_0} and q_{i_f}, $i = 1, 2, 3$. The parameters of the function, both in the simulation and experiments, φ_i are calculated at $t_0 = 0.1$ s, while the final time is $t_f = 2$ s. Moreover, to verify the robustness properties of the controller in simulation, random noise with uniform distribution $\boldsymbol{\eta} = [\eta_1\ \eta_2\ \eta_3]^T$ with the following upper bounds, determined by signal processing methods during experimental tests has been added to the angular accelerations of the joints

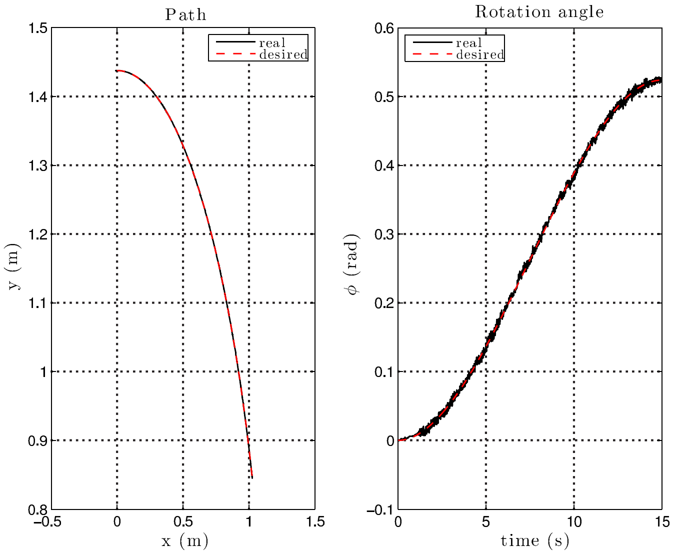

Fig. 8. (Left) Path and (right) rotation angle of the end-effector ϕ on the plane (experimental results).

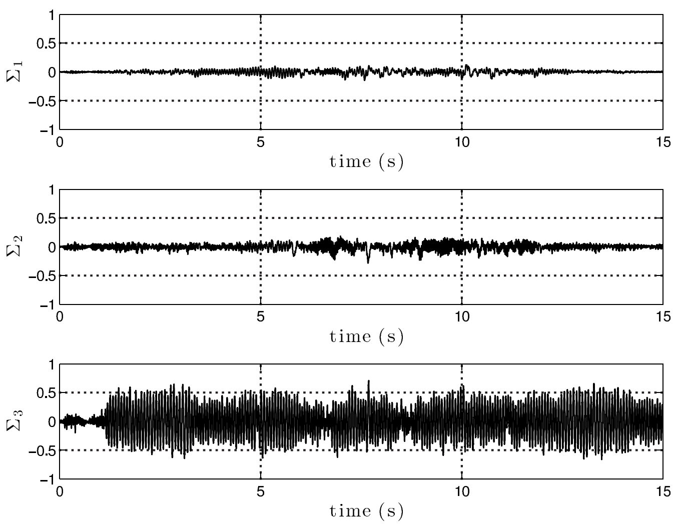

Fig. 9. Auxiliary sliding variable Σ_i for joints 1–3, respectively (experimental results).

of the simulated robot:

$$|\eta_1| \leq 20 \tag{40}$$

$$|\eta_2| \leq 80 \tag{41}$$

$$|\eta_3| \leq 100. \tag{42}$$

Figs. 7–10, respectively, show the time evolution of the joint variables, the end-effector position and orientation angle ϕ, the corresponding auxiliary sliding variables Σ_i (maintained to zero from the initial time instant), and the sliding variables s_i steered to zero in the prescribed finite time $t_f = 2$ s. In Fig. 11, the joints tracking errors are reported. The experimental results are satisfactory. The proposed control approach has demonstrated to be robust and precise, as expected theoretically, also in practice. This is confirmed by the extremely low root mean square (rms) tracking error, i.e., $e_{\text{RMS}} = 9.0477 \times 10^{-5}$ rad.

Finally, it is useful to compare our proposal with already published approaches, relying on the experimental results. To this end, the proposed control strategy, described in Section III, is compared with the classical PD control [36] and with the basic SSOSM control [24], by confronting the corresponding tracking errors for each joint (Fig. 12) and by computing for each approach the rms value of the tracking error norm

$$\|\boldsymbol{e}\|_{\text{RMS}} = \sqrt{\frac{1}{N}\sum_{k=1}^{N}\|\boldsymbol{e}(k)\|^2} \tag{43}$$

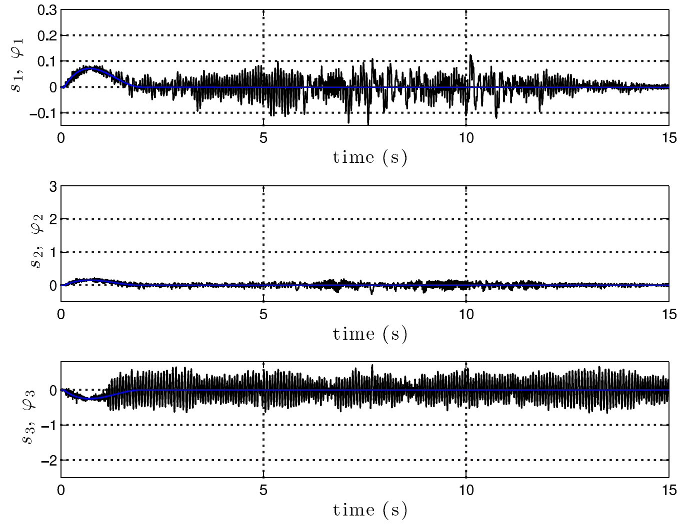

Fig. 10. Sliding variable s_i (solid black line) and the transient function φ_i (solid blue line) for joints 1–3, respectively (experimental results).

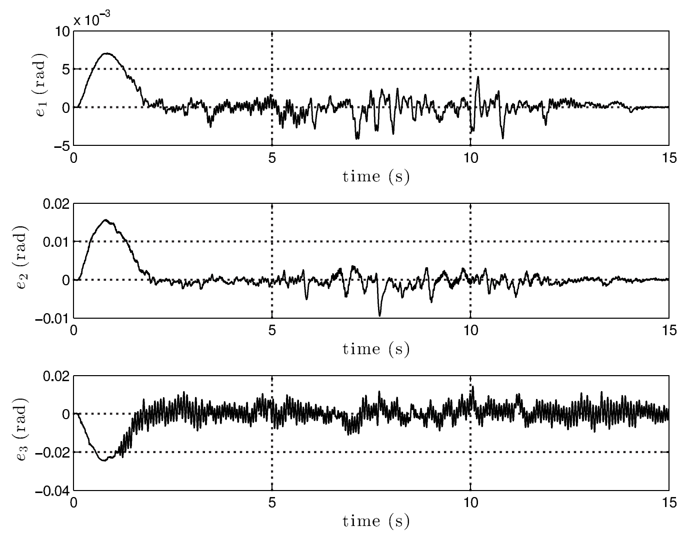

Fig. 11. Tracking error for each joint using ISSOSM control (experimental results).

TABLE III

COMPARISON OF THE RMS VALUE OF TRACKING ERROR NORM FOR THE CONSIDERED CONTROLLERS: PD, SSOSM, AND ISSOSM (EXPERIMENTS)

Control	$\|\boldsymbol{e}\|_{RMS}$
PD	0.016
SSOSM	0.0056
ISSOSM	0.0037

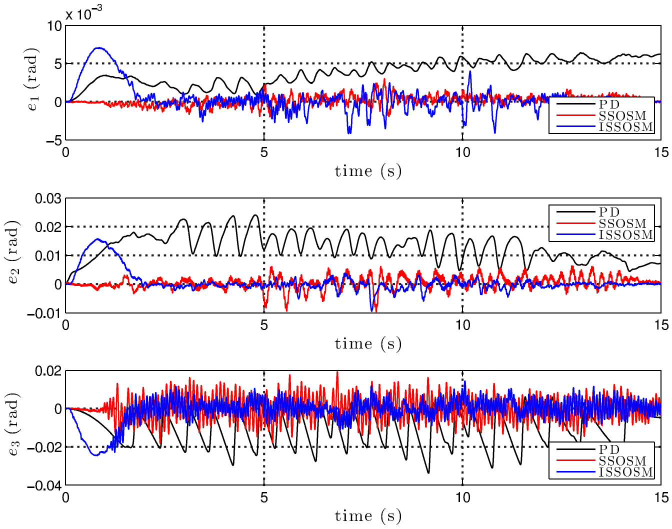

Fig. 12. Tracking error for each joint using PD, SSOSM, and ISSOSM control (experimental results).

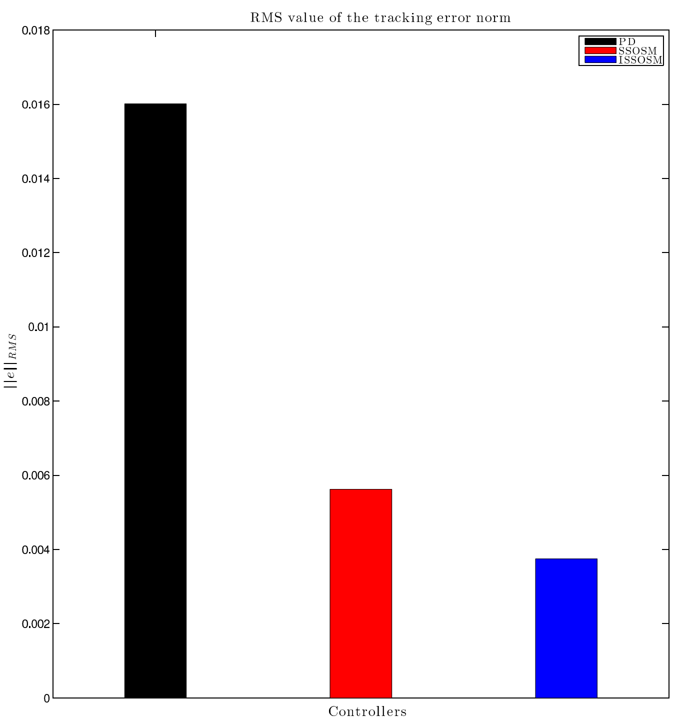

Fig. 13. RMS value of the tracking error norm for three compared robot control approaches: PD (black), SSOSM (red), and ISSOSM (blue) control (experimental results).

with $\boldsymbol{e}$ as in (32) and N equal to the number of sampling steps of the experiments. As for $\|\boldsymbol{e}\|_{\mathrm{RMS}}$, the results are shown in Table III and graphically rendered in Fig. 13. It is apparent that the proposed algorithm outperforms the other two. The reason for this has to be searched in the augmented robustness guaranteed by the reduction of the reaching phase, as proved theoretically in Theorem 2. Note that a possibility to further improve the performance, avoiding possible high accelerations and torques, could be that of explicitly including constraints on ξ_{1_i}, ξ_{2_i} in the SMC design, in analogous with that in [37].

V. Conclusion

In this paper, the good features of the ISM control approach are extended to the so-called suboptimal algorithm. A new version of such an algorithm, named ISSOSM algorithm, has been formulated. Some theoretical results have been first discussed: the finite time regulation of the auxiliary system state, the reduction of the reaching phase, as well as the robustness of the proposed approach, which turns out to be guaranteed since the initial time instant. Then, to assess the practical applicability of the proposal, the new algorithm has been used to design a motion control scheme for robot manipulators. The scheme has been tested experimentally, relying on a real industrial robot. The effectiveness of the proposed algorithm in terms of convergence and robustness is confirmed by the satisfactory experimental results. In addition, the proposed algorithm has been compared, experimentally, with other algorithms for robot control: the traditional PD control and the original version of the suboptimal algorithm. The comparison is reasonably fair since the parameters of the three algorithms have been calibrated to the best of our abilities. Indeed, all the algorithms perform in an acceptable way, but the one proposed in this paper, thanks to its enhanced robustness, clearly outperforms the others.

Acknowledgment

The authors would like to thank the Senior Lab Technician G. De Felici for the contribution and the full help provided during the experimental tests.

References

[1] V. I. Utkin, *Sliding Modes in Control Optimization*. New York, NY, USA: Springer-Verlag, 1992.

[2] C. Edwards and S. K. Spurgeon, *Sliding Mode Control: Theory and Applications*. London, U.K.: Taylor & Francis, 1998.

[3] L. Fridman, "Singularly perturbed analysis of chattering in relay control systems," *IEEE Trans. Autom. Control*, vol. 47, no. 12, pp. 2079–2084, Dec. 2002.

[4] I. Boiko, L. Fridman, A. Pisano, and E. Usai, "Analysis of chattering in systems with second-order sliding modes," *IEEE Trans. Autom. Control*, vol. 52, no. 11, pp. 2085–2102, Nov. 2007.

[5] A. Levant, "Chattering analysis," *IEEE Trans. Autom. Control*, vol. 55, no. 6, pp. 1380–1389, Jun. 2010.

[6] I. M. Boiko, "Analysis of chattering in sliding mode control systems with continuous boundary layer approximation of discontinuous control," in *Proc. Amer. Control Conf.*, San Francisco, CA, USA, Jun./Jul. 2011, pp. 757–762.

[7] M. W. Spong, S. Hutchinson, and M. Vidyasagar, *Robot Modeling and Control*. New York, NY, USA: Wiley, 2005.

[8] A. Ferrara and L. Giacomini, "Control of a class of mechanical systems with uncertainties via a constructive adaptive/second order VSC approach," *J. Dyn. Syst., Meas., Control*, vol. 122, no. 1, pp. 33–39, 2000.

[9] A. Ferrara, L. Magnani, and R. Scattolini, "A switching scheme for mixed PZT-based/jet thrusters control of a large flexible structure," *J. Dyn. Syst., Meas., Control*, vol. 123, no. 4, pp. 722–727, 2001.

[10] A. Ferrara and C. Lombardi, "Interaction control of robotic manipulators via second-order sliding modes," *Int. J. Adapt. Control Signal Process.*, vol. 21, nos. 8–9, pp. 708–730, 2007.

[11] A. Ferrara and M. Rubagotti, "Second-order sliding-mode control of a mobile robot based on a harmonic potential field," *IET Control Theory Appl.*, vol. 2, no. 9, pp. 807–818, Sep. 2008.

[12] J. Davila, L. M. Fridman, and A. Levant, "Second-order sliding-mode observer for mechanical systems," *IEEE Trans. Autom. Control*, vol. 50, no. 11, pp. 1785–1789, Nov. 2005.

[13] J. Davila, L. M. Fridman, and A. Poznyak, "Observation and identification of mechanical systems via second order sliding modes," *Int. J. Control*, vol. 79, no. 10, pp. 1251–1262, 2006.
[14] E. Cruz-Zavala, J. A. Moreno, and L. M. Fridman, "Uniform second-order sliding mode observer for mechanical systems," in *Proc. 11th Int. Workshop Variable Struct. Syst. (VSS)*, Mexico City, Mexico, Jun. 2010, pp. 14–19.
[15] G. Bartolini, A. Ferrara, and E. Usai, "Output tracking control of uncertain nonlinear second-order systems," *Automatica*, vol. 33, no. 12, pp. 2203–2212, Dec. 1997.
[16] G. Bartolini, A. Ferrara, E. Usai, and V. I. Utkin, "On multi-input chattering-free second-order sliding mode control," *IEEE Trans. Autom. Control*, vol. 45, no. 9, pp. 1711–1717, Sep. 2000.
[17] G. Bartolini, A. Ferrara, and E. Usai, "Chattering avoidance by second-order sliding mode control," *IEEE Trans. Autom. Control*, vol. 43, no. 2, pp. 241–246, Feb. 1998.
[18] A. Levant, "Higher-order sliding modes, differentiation and output-feedback control," *Int. J. Control*, vol. 76, nos. 9–10, pp. 924–941, Jan. 2003.
[19] A. Levant, "Quasi-continuous high-order sliding-mode controllers," *IEEE Trans. Autom. Control*, vol. 50, no. 11, pp. 1812–1816, Nov. 2005.
[20] T. Floquet, J.-P. Barbot, and W. Perruquetti, "Higher-order sliding mode stabilization for a class of nonholonomic perturbed systems," *Automatica*, vol. 39, no. 6, pp. 1077–1083, Jun. 2003.
[21] F. Dinuzzo and A. Ferrara, "Higher order sliding mode controllers with optimal reaching," *IEEE Trans. Autom. Control*, vol. 54, no. 9, pp. 2126–2136, Sep. 2009.
[22] V. I. Utkin, J. Guldner, and J. Shi, *Sliding Mode Control in Electro-Mechanical Systems*. London, U.K.: Taylor & Francis, 1999.
[23] G. Bartolini, A. Pisano, E. Punta, and E. Usai, "A survey of applications of second-order sliding mode control to mechanical systems," *Int. J. Control*, vol. 76, nos. 9–10, pp. 875–892, Jan. 2003.
[24] L. M. Capisani, A. Ferrara, and L. Magnani, "Design and experimental validation of a second-order sliding-mode motion controller for robot manipulators," *Int. J. Control*, vol. 82, no. 2, pp. 365–377, Jan. 2009.
[25] L. M. Capisani and A. Ferrara, "Trajectory planning and second-order sliding mode motion/interaction control for robot manipulators in unknown environments," *IEEE Trans. Ind. Electron.*, vol. 59, no. 8, pp. 3189–3198, Aug. 2012.
[26] L. M. Capisani, T. Facchinetti, and A. Ferrara, "Real-time networked control of an industrial robot manipulator via discrete-time second-order sliding modes," *Int. J. Control*, vol. 83, no. 8, pp. 1595–1611, Jul. 2010.
[27] A. Levant and L. Alelishvili, "Integral high-order sliding modes," *IEEE Trans. Autom. Control*, vol. 52, no. 7, pp. 1278–1282, Jul. 2007.
[28] A. Levant, "Robust exact differentiation via sliding mode technique," *Automatica*, vol. 34, no. 3, pp. 379–384, Mar. 1998.
[29] A. Levant, "Homogeneity approach to high-order sliding mode design," *Automatica*, vol. 41, no. 5, pp. 823–830, May 2005.
[30] A. Ferrara and G. P. Incremona, "Robust motion control of a robot manipulator via integral suboptimal second order sliding modes," in *Proc. IEEE 52nd Conf. Decision Control*, Dec. 2013, pp. 1107–1112.
[31] J. P. Aubin and A. Cellina, *Differential Inclusions*. Berlin, Germany: Springer-Verlag, 1984.
[32] A. Levant, "Sliding order and sliding accuracy in sliding mode control," *Int. J. Control*, vol. 58, no. 6, pp. 1247–1263, Dec. 1993.
[33] G. Bartolini, A. Ferrara, and E. Usai, "On boundary layer dimension reduction in sliding mode control of SISO uncertain nonlinear systems," in *Proc. IEEE Int. Conf. Control Appl.*, vol. 1. Trieste, Italy, Sep. 1998, pp. 242–247.
[34] V. I. Utkin and J. Shi, "Integral sliding mode in systems operating under uncertainty conditions," in *Proc. 35th IEEE Conf. Decision Control*, vol. 4. Kobe, Japan, Dec. 1996, pp. 4591–4596.
[35] A. Calanca, L. M. Capisani, A. Ferrara, and L. Magnani, "MIMO closed loop identification of an industrial robot," *IEEE Trans. Control Syst. Technol.*, vol. 19, no. 5, pp. 1214–1224, Sep. 2011.
[36] B. Siciliano, L. Sciavicco, L. Villani, and G. Oriolo, *Robotics: Modelling, Planning and Control*, 3rd ed. London, U.K.: Springer-Verlag, 2009.
[37] M. Rubagotti and A. Ferrara, "Second order sliding mode control of a perturbed double integrator with state constraints," in *Proc. Amer. Control Conf.*, Baltimore, MD, USA, Jun. 2010, pp. 985–990.

Antonella Ferrara (SM'03) is currently a Full Professor of Automatic Control with the University of Pavia, Pavia, Italy. She has authored or co-authored over 290 papers, including more than 90 journal papers. Her current research interests include sliding mode and nonlinear control with application to traffic, automotive, and robotics.

Prof. Ferrara is a Senior Member of the IEEE Control Systems Society, and a member of the IEEE Technical Committee on Variable Structure and Sliding Mode Control, the IEEE Robotics and Automation's Technical Committee on Autonomous Ground Vehicles and Intelligent Transportation Systems, and the IFAC Technical Committee on Transportation Systems. Since 2013, she has been the Chair of the Women in Control Standing Committee of the Control Systems Society. She was an Associate Editor of the IEEE TRANSACTIONS ON CONTROL SYSTEMS TECHNOLOGY and the IEEE TRANSACTIONS ON AUTOMATIC CONTROL. Since 2014, she has been an Associate Editor of the *IEEE Control Systems Magazine*.

Gian Paolo Incremona (M'10) received the master's (Hons.) degree in electrical engineering from the University of Pavia, Pavia, Italy, in 2012, where he is currently pursuing the Ph.D. degree in electronics, electrical and computer engineering with the Identification and Control of Dynamic Systems Laboratory.

He was a student with Almo Collegio Borromeo, Pavia, and the Class of Science and Technology, Institute for Advanced Study of Pavia, Pavia. His current research interests include industrial robotics, real-time physical systems, optimal control, and variable structure control methods of sliding mode type.